



HAL
open science

A simplified Youla-Kučera parametrized adaptive feedforward compensator for active vibration and noise control with internal coupling

Ioan Doré Landau, Tudor-Bogdan Airimitoiaie, Raul Meléndez, Luc Dugard

► To cite this version:

Ioan Doré Landau, Tudor-Bogdan Airimitoiaie, Raul Meléndez, Luc Dugard. A simplified Youla-Kučera parametrized adaptive feedforward compensator for active vibration and noise control with internal coupling. 2020. hal-02556162

HAL Id: hal-02556162

<https://hal.science/hal-02556162>

Preprint submitted on 27 Apr 2020

HAL is a multi-disciplinary open access archive for the deposit and dissemination of scientific research documents, whether they are published or not. The documents may come from teaching and research institutions in France or abroad, or from public or private research centers.

L'archive ouverte pluridisciplinaire **HAL**, est destinée au dépôt et à la diffusion de documents scientifiques de niveau recherche, publiés ou non, émanant des établissements d'enseignement et de recherche français ou étrangers, des laboratoires publics ou privés.

A simplified Youla-Kučera parametrized adaptive feedforward compensator for active vibration and noise control with internal coupling

Ioan Doré Landau^{a,*}, Tudor-Bogdan Airimițoae¹, Raul Melendez^a, Luc Dugard^a

^aUniv. Grenoble Alpes, CNRS, Grenoble INP, GIPSA-lab, 38000 Grenoble, France

^bUniv. Bordeaux, Bordeaux INP, CNRS, IMS, UMR 5218, 33405 Talence, France

Abstract

In [7] a Finite Impulse Response (FIR) Youla-Kučera (YK) parametrized adaptive feedforward compensator has been introduced for active vibration control with mechanical coupling. The same configuration can also be used for active noise control with acoustical coupling. The major advantage of this scheme is the possibility to guarantee the stability of the internal positive feedback loop independently of the evolution of the adaptive parameters of the YK filter which will be tuned in order to minimize the residual error. The stability of the global scheme will however depend on the satisfaction of a strictly positive real (SPR) condition. It is shown in this note that a particular choice for the central stabilizing filter used in YK parametrization will drastically simplify the implementation of the algorithm without affecting the performance. This will be illustrated experimentally by the results on an active noise control system with acoustic coupling.

Keywords: active vibration control, active noise control, adaptive feedforward compensation, adaptive control, Youla-Kučera parametrization,

1. Introduction

Adaptive active feedforward compensation of noise and vibrations is widely used when a signal correlated with the disturbance (image of the disturbance) is available. Unfortunately an internal positive coupling between the feedforward compensation and the measurement of the image of the disturbance occurs in most of the applications of adaptive feedforward compensation schemes for active noise and vibration control (ANVC) [8],[3]. This often leads to the instability of the system [5],[4]. Figure 1 gives the basic block diagram of the adaptive feedforward compensation in the presence of the internal positive coupling between the output of the compensator and the measurement of the image of the incoming disturbance. The incoming disturbance propagates through the so called *primary path* D and its effect is compensated by a secondary source (sound or force) through the *secondary path* G driven by a feedforward compensator N . The input to the feedforward compensator is the sum of the image of the incoming disturbance and of the internal acoustical or mechanical positive feedback M . This unwanted coupling raises problems in practice and makes the analysis of adaptive algorithms more difficult. The residual noise or acceleration χ^0 is used to emulate the adaptation of the feedforward compensator in order to take into account the unknown characteristics of the disturbance. The dynamics characteristics of the system are almost constant and models of the system are obtained by identification from experimental

data.

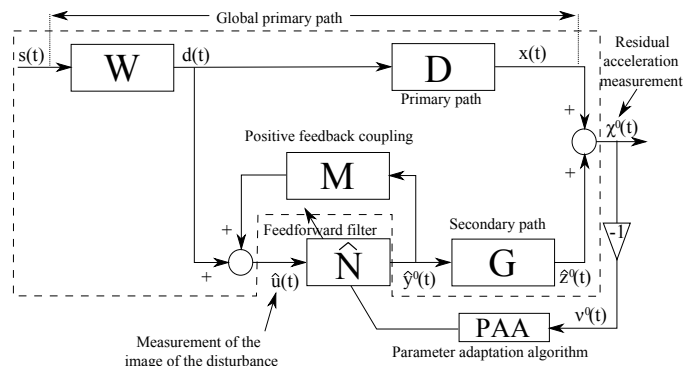


Figure 1: Feedforward ANVC with adaptive feedforward compensator.

In [7] a Finite Impulse Response (FIR) Youla-Kučera (YK) parametrized feedforward compensator has been introduced for active vibration control with mechanical coupling. The motivation for the introduction of the FIR Youla-Kučera parametrization was the separation of the stabilization of the “internal” positive feedback loop created by the internal coupling from the adaptation of the FIR YK filter parameters in order to minimize the residual error (acceleration). The same configuration can also be used for active noise control with acoustical coupling. The major advantage of this scheme is the possibility to guarantee the stability of the internal positive feedback loop independently of the evolution of the adaptive parameters of the YK filter. The stability of the global scheme will however depend

*This paper was not presented at any IFAC meeting. Corresponding author I. D. Landau. Tel. +33-4-7682-6391. E-mail: ioan-dore.landau@gipsa-lab.grenoble-inp.fr.

One defines also a filtered observation vector:

$$\phi_f(t) = L(q^{-1})\phi(t) = [\alpha_f(t+1), \alpha_f(t), \dots, \alpha_f(t-n_Q+1)] \quad (13)$$

where

$$\alpha_f(t+1) = L(q^{-1})\alpha(t+1) \quad (14)$$

and $L(q^{-1})$ is an asymptotically stable filter.

The following parameter adaptation algorithm is used:

$$\hat{\theta}(t+1) = \hat{\theta}(t) + F(t)\Phi(t)v(t+1); \quad (15)$$

$$v(t+1) = \frac{v^0(t+1)}{1 + \Phi^T(t)F(t)\Phi(t)}; \quad (16)$$

$$F(t+1) = \frac{1}{\lambda_1(t)} \left[F(t) - \frac{F(t)\Phi(t)\Phi^T(t)F(t)}{\lambda_1(t) + \Phi^T(t)F(t)\Phi(t)} \right] \quad (17)$$

$$1 \geq \lambda_1(t) > 0; 0 \leq \lambda_2(t) < 2; F(0) > 0 \quad (18)$$

$$\Phi(t) = \phi_f(t) \quad (19)$$

where $\lambda_1(t)$ and $\lambda_2(t)$ allow to obtain various time profiles for the matrix adaptation gain $F(t)$ (see [6]).

In the context of this paper we will be interested by two types of adaptation gain allowing to operate in an "adaptive" regime.

- *Constant trace algorithm.* $\lambda_1(t)$ and $\lambda_2(t)$ are adjusted continuously to maintain constant the trace of the adaptation gain matrix. This allows to move in the optimal direction while maintaining the adaptation capabilities. The values of $\lambda_1(t)$ and $\lambda_2(t)$ in order to maintain constant the trace of the adaptation gain matrix are determined from the equation:

$$\text{tr}(F(t+1)) = \frac{1}{\lambda_1(t)} \text{tr} \left(F(t) - \frac{F(t)\Phi(t)\Phi^T(t)F(t)}{\delta(t) + \Phi^T(t)F(t)\Phi(t)} \right)$$

fixing the ratio $\delta(t) = \lambda_1(t)/\lambda_2(t) = \text{const.}$ Typical value: $\delta = 1$.

- *Constant scalar adaptation gain.* This is obtained by taking $\lambda_1(t) \equiv 1$, $\lambda_2(t) \equiv 0$ and $F(t) = \gamma I$, $\gamma > 0$ where I is the identity matrix.

Two choices for the filter L will be considered, leading to two different algorithms (see [7] for details).

Algorithm II $L = \hat{G}$

Algorithm III

$$L = \frac{\hat{A}_M}{\hat{P}} \hat{G} \quad (20)$$

where :

$$\hat{P} = \hat{A}_M S_0 - \hat{B}_M R_0 \quad (21)$$

is an estimation of the polynomial defining the closed loop poles of the internal loop. The equation of the a posteriori adaptation error $v(t+1)$ obeys an equation of the form:

$$v(t+1) = H(q^{-1})[\theta - \hat{\theta}(t+1)]^T \Phi(t) \quad (22)$$

where :

$$H(q^{-1}) = \frac{A_M(q^{-1})G(q^{-1})}{P(q^{-1})L(q^{-1})}, \Phi = \phi_f \quad (23)$$

and the stability condition is

$$H'(z^{-1}) = H(z^{-1}) - \frac{\lambda_2}{2}, \max_t [\lambda_2(t)] \leq \lambda_2 < 2 \quad (24)$$

should be strictly positive real (SPR)². For Algorithm II this condition is:

$$H(q^{-1}) = \frac{A_M(q^{-1})G(q^{-1})}{P(q^{-1})\hat{G}(q^{-1})} - \frac{\lambda_2}{2}, \max_t [\lambda_2(t)] \leq \lambda_2 < 2 \quad (25)$$

should be SPR and for Algorithm III one has:

$$H(q^{-1}) = \frac{A_M}{\hat{A}_M} \cdot \frac{\hat{P}}{P} \cdot \frac{G}{\hat{G}} - \frac{\lambda_2}{2}, \max_t [\lambda_2(t)] \leq \lambda_2 < 2 \quad (26)$$

should be SPR. It is clear from (26) that for any stable P using Algorithm III one always can satisfy the SPR condition provided that the estimations of M and G are enough good (which is the case in practice). The term "enough good" is interpreted as the condition that the phase difference between the true model ($A_M G/P$) and the estimated model $\hat{A}_M \hat{G}/\hat{P}$ is between -90° and $+90^\circ$ at all frequencies which assures the satisfaction of the SPR condition for constant scalar adaptation gain. This condition is slightly sharper for the constant trace algorithm. However in many situations, for the Algorithm II the SPR condition will be violated over a certain frequency range and even the averaging arguments [2] may not be applicable for the relaxation of the stability condition. If the objective is only to design a stabilizing central filter (which is generally the case), one can make the choice $P = A_M$ by choosing $R_0 = 0, S_0 = 1$ ($\hat{P} = \hat{A}_M$)³. With this choice, both algorithms become the same and the stability condition will be:

$$H(q^{-1}) = \frac{G}{\hat{G}} - \frac{\lambda_2}{2}, \max_t [\lambda_2(t)] \leq \lambda_2 < 2 \quad (27)$$

should be SPR. This condition will be always satisfied provided that one has a good estimation of the model of the secondary path \hat{G} . This leads to a drastic simplification of the central stabilizing filter which using pole placement will have at least $n_{A_G} + n_{B_G} + d_G$ parameters⁴. There is also a drastic simplification in the filter L by suppressing the term \hat{A}_M/\hat{P} which has $2n_{A_M} + 1 + n_{B_M} + d_M$ parameters. Since the orders of the models in active vibration and noise control are high, the reduction of the number of parameters is significant.

4. Experimental results

The view of the active noise control test-bench used for experiments is shown in Fig. 3 and its detailed scheme is given in Fig. 4.

²For the constant scalar adaptation gain $\lambda_2 = 0$ and this is valid for all the subsequent stability conditions

³This assumes that the compensation path is asymptotically stable, which indeed is the case in practice

⁴One has to associate a multiplication and an addition for each parameter

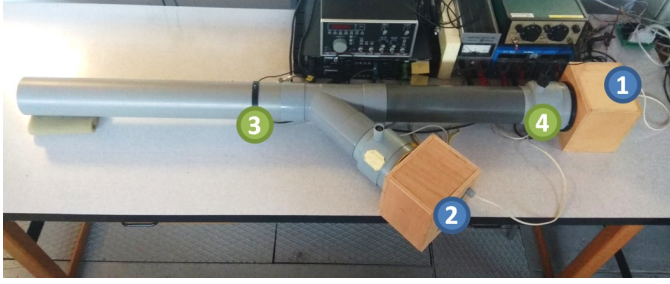


Figure 3: Duct active noise control test-bench (Photo).

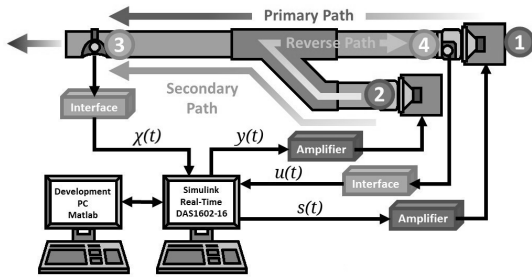


Figure 4: Duct active noise control test-bench diagram.jpg

The speaker used as the source of disturbances is labeled as 1, while the control speaker is marked as 2. At pipe's open end, the microphone that measures the system's output (residual noise $\chi(t)$) is denoted as 3. $s(t)$ is the disturbance. Inside the pipe, close to the source of disturbances, the second microphone, labeled as 4, measures the perturbation's image, denoted as $u(t)$. $y(t)$ is the control signal. The transfer function between the disturbance's speaker and the microphone (1→3) is called *Global Primary Path*, while the transfer function between the control speaker and the microphone (2→3) is denoted *Secondary Path*. The transfer function between microphones (4→3) is called *Primary Path*. The internal coupling found between (2→4) is denoted *Reverse Path*. These marked paths have a double differentiator behavior, since as input we have the voice coil displacement and as output the air acoustical pressure. Speakers and microphones are connected to an xPC

Model	n_A	n_B	d
Global primary path	24	20	7
Secondary path	26	27	6
Reverse path	25	22	5

Table 1: Orders of the identified models.

Target computer with Simulink Real-time[®]. A second computer is used for development and operation with Matlab. Taking into account that disturbances up to 400 Hz may need to be attenuated, a sampling frequency $f_s = 2500$ Hz has been chosen ($T_s = 0.0004$ sec). The orders of the identified models are summarized in Table 1. The frequency characteristics of the iden-

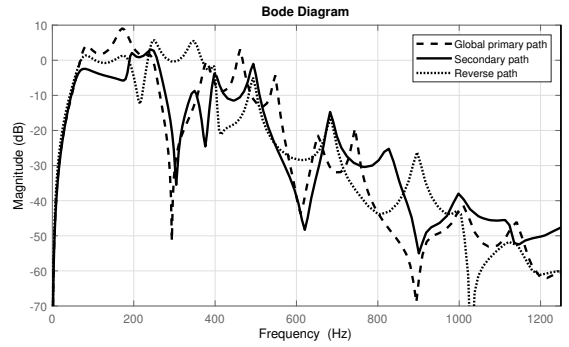


Figure 5: Frequency characteristics of the Global primary, Secondary and Reverse paths identified models.

Adaptation algorithm	Attenuation [dB]
Matrix (Alg. III)	27.0
Matrix (Alg. II)	unstable
Scalar (Alg. III)	26.7
Scalar (Alg. II)	unstable

Table 2: Experimental results for FIRYK 60/0 adaptive compensators (70-270 Hz broad-band disturbance, 180 s experiments).

tified models for the global primary⁵, secondary and reverse paths are shown in Fig. 5. These characteristics present multiple resonances (low damped complex poles)⁶ and anti-resonances (low damped complex zeros). One can see that the secondary

Adaptation algorithm	Attenuation [dB]
Matrix (Alg.II/Alg. III)	27.19
Scalar (Alg.II/Alg. III)	27.17

Table 3: Experimental results for simplified FIRYK 60/0 adaptive compensators (70-270 Hz broad-band disturbance, 180 s experiments).

path has a high gain between 70 to 270 Hz which means that disturbances can be efficiently attenuated in this zone. It is also clear that the reverse path has a significant gain on a large frequency range (up to 400 Hz) so its effect can not be neglected.

A broad band disturbance located between 70 and 270 Hz is considered as an unknown disturbance. Table 2 gives a comparison of the various adaptation algorithms in terms of global attenuation for a FIRYK adaptive compensator with 60 adaptive parameters. Results are given for scalar and matrix adaptation gains. In this case the poles of the internal loop are different from the poles of the A_M (the central controller has 59 parameters resulting from the solution of a Bezout equation). It was observed that the Alg.II is unstable and this can be understood when looking to the phase plot of the estimated $\frac{A_M}{P}$ given in Figure 6. It can be observed that $\frac{A_M}{P}$ is not positive real in a

⁵The global primary path model has been exclusively used for simulation purposes.

⁶The lowest damping is around 0.01.

large frequency range from 110 Hz to 760 Hz⁷ and one absolutely needs to use the Algorithm III. Table 3 gives the comparison of the various algorithms as in Table 2 but for the case $P = A_M$ with $R_0 = 0, S_0 = 1$ ($\hat{P} = \hat{A}_M$). As expected both algorithms will give the same results and the performance is similar to that of the Alg. III in Table 2. In this case 59 parameters in the central filter and 78 parameters in the filter L have been suppressed. Figure 7 gives the evolution of the residual noise in the case $P \neq A_M$ for a matrix adaptation gain and Figure 8 gives the evolution of the residual noise for the case $P = A_M$ and a matrix adaptation gain. The behaviour is similar for the two cases. Figure 9 gives the power spectral density for the two cases in steady state. In the region of interest(70-270 Hz) they are extremely close.

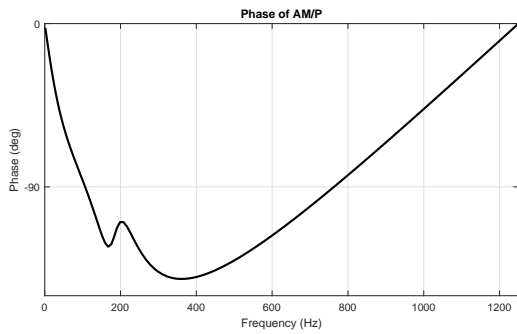


Figure 6: Phase of $\frac{A_M}{P}$ for the FIRYK 60/0 adaptive compensator (70-270 Hz disturbance).

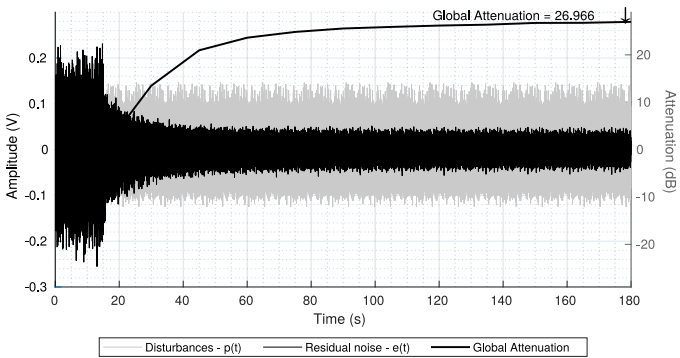


Figure 7: Residual noise using the complete FIRYK 60/0 adaptive compensators ($P \neq A_M$) with FUSBA matrix adaptation (70-270 Hz disturbance).

5. Conclusion

A drastic simplification of the FIR Youla Kucera adaptive feedforward compensator for active control with internal coupling is obtained by choosing the poles of the internal closed loop equal to the poles of the reverse path. The performance obtained on a duct silencer are comparable with those for other

⁷Averaging can not be used since the region of non positive realness is much larger than the region where $\frac{A_M}{P}$ is SPR even within the range 70 - 270 Hz.

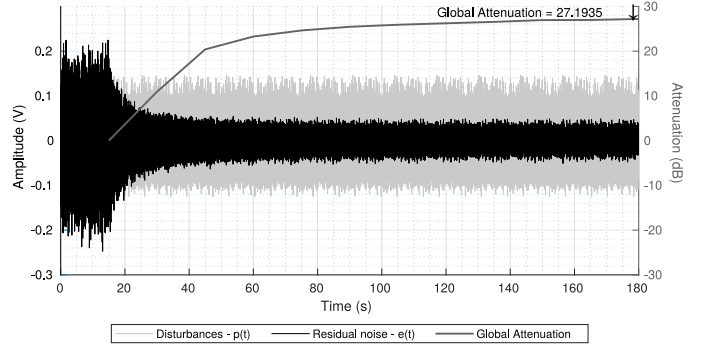


Figure 8: Residual noise using the simplified FIRYK 60/0 adaptive compensators ($P = A_M$) with FUPLR/FUSBA matrix adaptation (70-270 Hz disturbance).

choices of the poles of the internal closed loop but with a significant reduction of the algorithm complexity and a simplification of the design of the central controller. This option should also lead to a relaxation of the SPR conditions for combined feed-forward/feed-back active control schemes [1].

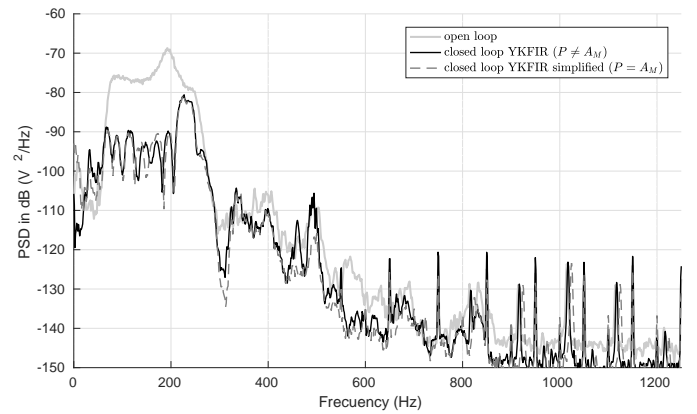


Figure 9: Power spectral density of the residual noise (70-270 Hz disturbance).

References

- [1] T.B. Airimitoie and I.D. Landau. Combined adaptive feedback and feed-forward compensation for active vibration control using Youla Kučera parametrization. *J. of Sound and Vibration*, 434:422 – 441, 2018.
- [2] B.D.O. Anderson, R.R. Bitmead, C.R. Johnson, P.V. Kokotovic, R.L. Kosut, I.M.Y. Mareels, L. Praly, and B.D. Riedle. *Stability of adaptive systems*. The M.I.T Press, Cambridge Massachusetts, London, England, 1986.
- [3] S. Elliott. *Signal processing for active control*. Academic Press, San Diego, California, 2001.
- [4] C.A Jacobson, C.R Johnson, D.C Mc Cormick, and W.A Sethares. Stability of active noise control algorithms. *IEEE Signal Processing letters*, 8(3):74–76, 2001.
- [5] M.S. Kuo and D.R. Morgan. *Active noise control systems- Algorithms and DSP implementation*. Wiley, New York., 1996.
- [6] I. D. Landau, R. Lozano, M. M'Saad, and A. Karimi. *Adaptive control*. Springer, London, 2nd edition, 2011.
- [7] I.D. Landau, T.B. Airimitoie, and M. Alma. A Youla-Kučera parametrized adaptive feedforward compensator for active vibration control with mechanical coupling. *Automatica*, 48(9):2152 – 2158, 2012.
- [8] J Zeng and R.A de Callafon. Recursive filter estimation for feedforward noise cancellation with acoustic coupling. *Journal of sound and vibration*, 291:1061–1079, 2006.